



# Geochemistry of Palaeoproterozoic Kajrahat Limestone, Vindhyan Supergroup, central India: insights into depositional conditions and sources of rare earth elements

Akanksha Singh<sup>1</sup> · B. P. Singh<sup>1</sup> · S. Kanhaiya<sup>2</sup> · M. A. Quasim<sup>3</sup> · A. Patra<sup>4</sup> · S. Singh<sup>5</sup> · V. K. Srivastava<sup>6</sup>

Accepted: 26 January 2024 / Published online: 9 March 2024

© The Author(s), under exclusive licence to Springer-Verlag GmbH Germany, part of Springer Nature 2024

## Abstract

The Lower Vindhyan (Semri) Group substantially consists of unmetamorphosed and undeformed sedimentary sequences of Palaeoproterozoic age. A detailed geochemical study has been carried out to infer the paleoenvironment and the source of REEs for the Palaeoproterozoic Kajrahat Limestone, Vindhyan Supergroup, Central India. This study investigates the geochemical composition of major, trace and rare earth elements (REEs). The studied limestones, have a high percentage of CaO (ranging from 30.87 to 48.59) implies that calcite was the primary mineral phase in these carbonates. SiO<sub>2</sub> is second most abundant major oxide. Sr is dominant trace element showing a negative correlation with CaO. All trace elements exhibit depletion with respect to Post-Archean Australian Shale (PAAS). The PAAS-normalized REE pattern of studied limestone has a relatively uniform pattern, with slightly enriched LREE compared to HREE with negative Ce anomaly. Collectively, low concentration of U and U/Th, Ce/Ce\* ratios clearly indicates an oxic depositional condition for the samples. The ΣREE shows a positive correlation with SiO<sub>2</sub>, TiO<sub>2</sub> and Al<sub>2</sub>O<sub>3</sub> ( $r^2 = 0.87, 0.84$  and  $0.91$  respectively) and a weak positive correlation with CaO ( $r^2 = 0.12$ ) suggested that siliciclastic sediments also serve as a source for the REEs beside seawater. This, in turn, indicates that the deposition of this limestone occurred in a coastal/shallow marine environment with some contribution from continental part.

**Keywords** Geochemistry · Palaeoproterozoic limestone · Depositional environment · Vindhyan Supergroup

## Introduction

One of the prime focus of sedimentological study is to decode ancient sedimentary environments, and the present study attempts to decode the depositional environment of Palaeoproterozoic Kajrahat Limestone of Central India. Characteristics of sedimentary rocks depend on formation, transport and depositional processes and include physical, chemical and biological factors in any depositional environment (Nichols 2009). Geochemistry is an important tool used in ascertaining the depositional imprints and overprints of post-depositional processes on sediments. The chemical composition of carbonate rocks helps to infer the physico-chemical conditions in the deposition basin. Major oxides and trace elements act as indicators, revealing the composition of the carbonate rocks and provide information about the environmental conditions during deposition (Srivastava and Singh 2018). The source of the chemical elements to the oceans are various such as river, wind, hydrothermal sources, groundwater, etc. (Martin and Whitfield 1983;

✉ A. Patra  
amitava.geol@gmail.com

<sup>1</sup> Department of Geology, Banaras Hindu University, Varanasi 221005, India

<sup>2</sup> Department of Earth and Planetary Sciences, V.B.S. Purvanchal University, Jaunpur 222003, India

<sup>3</sup> Department of Geology, Aligarh Muslim University, Aligarh 202002, India

<sup>4</sup> Department of Geology, Nagaland University, Kohima Campus, Nagaland 797004, India

<sup>5</sup> Department of Geology, IEES, Dr. Rammanohar Lohia Avadh University, Ayodhya 224001, India

<sup>6</sup> Department of Geology, University of Lucknow, Lucknow 226007, India

Birgel et al. 2011; Coimbra et al. 2015). Carbonate deposition and seafloor redox dynamics act as depositional sinks because major and trace elements are incorporated into the calcium carbonate lattice, as seen in modern neritic and oceanic environments (Takematsu et al. 1993). Therefore major oxides and trace elements act as indicators of depositional environment of carbonate rocks. The low solubility of rare earth elements (REEs) in seawater means they are entirely incorporated into clastic sediments due to their short residence time in the water. Additionally, REEs tend to remain immobile during subsequent processes like diagenesis (Chaudhuri and Cullers 1979; Gong et al. 2018) and metamorphism (Muecke et al. 1979), chemical weathering and transport (Yang et al. 2017). Consequently, REE concentrations in ancient carbonate rocks serve to distinguish the sources of REEs, whether they originate from marine or non-marine milieu (Banner et al. 1988; Frimmel 2009; Zhao et al. 2009). The average provenance compositions can potentially be determined through REE patterns (Taylor and McLennan 1985; Bakkiaraj et al. 2010). Carbonate rocks typically contain low concentrations of REEs (Goldberg et al. 1963; Haskin and Haskin 1966; Tlig and M'Rabet 1985; Nogueira et al. 2019) and the distribution of REEs in these rocks is mostly affected by the conditions of deposition (Murray et al. 1990, 1992; Patra and Singh 2017; Srivastava and Singh 2018) and diagenetic processes (Scherer and Seitz 1980; Schieber 1988; Armstrong-Altrin et al. 2003; Morad et al. 2010; Fu et al. 2011). REEs are useful for determining the type of depositional environments including widespread marine anoxia (Liu et al. 1988; German and Elderfield 1990), oceanic palaeo-redox conditions (Wang et al. 1986; Elderfield and Pagett 1986; Kato et al. 2002), changes in surface productivity (Toyoda et al. 1990), distance from the source area (Murray et al. 1991), lithology and diagenesis (German and Elderfield 1990; Nath et al. 1992; Madhavaraju and Lee 2009) and palaeogeography and depositional models (Kamber and Webb 2001; Kemp and Trueman 2003).

Examining rare earth elements (REEs), mainly LREE, in sedimentary rocks offers insights into the initial composition of seawater. As a result, ancient sedimentary rocks have been recognized as trustworthy sources for REE proxies (Holser 1997). The Rare Earth Elements (REEs) in carbonate rocks preserved valuable information on paleo-seawater chemistry and local–regional redox conditions (Zhang and Shields 2023). REEs are substituted for  $\text{Ca}^{2+}$  in the carbonate lattice. It is believed that REEs exhibit greater stability compared to oxygen or carbon isotopes in the carbonate lattice during diagenetic processes (Zhong and Mucci 1995). Furthermore, diagenetic fluids typically exhibit low concentrations of REEs ranging from  $10^{-6}$  to  $10^{-4}$  ppm (Sholkovitz et al. 1989; Banner and Hanson 1990). Consequently, REE concentrations in ancient carbonate rocks are likely to remain unchanged, even during periods of considerable diagenesis

(Webb and Kamber 2000; Frimmel 2009). Seawater REE patterns found in marine chemical sediments, regardless of their age of deposition, show a uniform LREE depletion; enrichment of La, depletion of Ce and slight enrichment of Gd, in shale-normalized patterns (Shields and Webb 2004; Bolhar and Kranendonk 2007; Zhang and Nozaki 1996).

The Indian subcontinent is crucial in both Columbian and Rodinian reconstructions (Li et al. 2008; Meert and Santosh 2017). It has numerous Proterozoic sedimentary basins, mostly undeformed and unmetamorphosed, holding potential clues to tectonic, climatic and biological evolution on Earth's Proterozoic Eon. Only a few studies, explore evidence for Proterozoic global events from the carbonate formations in these basins (e.g., Ray et al. 2003; Mohanty et al. 2015; Ansari et al. 2018; George et al. 2018; Choudhuri et al. 2023). The Vindhyan Basin provides most of the data, boasting the largest Proterozoic sedimentary sequence in India. Ray et al. (2002, 2003) analyzed isotope systematic in carbonate sequences of the Vindhyan Supergroup, India to explore their geological significance, and age. According to their study of Pb–Pb dating and Sr isotope stratigraphy established the Kajrahat Limestone as Palaeoproterozoic age ( $1600 \pm 130$  Ma). Furthermore, there has been an investigation into the depositional environment by stable isotope composition of the Kajrahat Limestone (Banerjee et al. 2007). Singh et al. (2020) have recorded soft sedimentary deformation structures (SSDs) in the Kajrahat Limestone and have envisaged that earthquakes might have occurred multiple times between 1700 and 1600 Ma in Central India. Furthermore, this implies that the Vindhyan Basin experienced instability and the seismicity was primarily a result of rift-related tectonics in this intra-cratonic basin. Even after years of research, a comprehensive study of the REE geochemistry of Palaeoproterozoic Kajrahat Limestone of Lower Vindhyan succession remains unavailable. Therefore, the present study major, trace and REEs geochemistry of Kajrahat Limestone are analyzed and their variations are recorded to gain insights into the physico-chemical conditions that were prevailed during formation of these carbonates of the Vindhyan Basin. This study aims to investigate the depositional setting, identify potential REE sources, and provide insights into the variations in Eu and Ce anomalies within the studied limestones. Additionally, this study will contribute to understand the seawater chemistry during Palaeoproterozoic times in Central India.

## Geological setting

The Vindhyan Supergroup of Central India records a considerable portion of Proterozoic time and holds the distinction of being the largest of the Proterozoic sedimentary basins in the Indian subcontinent, known as the Purana

Basins (Kale and Phansalkar 1991). This sedimentary basin holds unmetamorphosed and slightly deformed layers that are approximately 4500 m thick. These beds have well-preserved sedimentary structures and provide evidence of paleo-environmental conditions during a significant portion of the Proterozoic eon (~ 1800–900 Ma) with good time resolution (Deb et al. 2002; Ray 2006; Malone et al. 2008; Gopalan et al. 2013). The Proterozoic Vindhyan Supergroup is found in Central India and covers an area of ~ 100,000 km<sup>2</sup>. A substantial portion of this Supergroup is concealed under the Gangatic alluvium and the Deccan traps (Gopalan et al. 2013). The western boundary of this Supergroup is defined by the Great Boundary Fault (GBF), while the southern limit is marked by the Narmada-Son lineament (Fig. 1A). These sequences have been found in two areas: the western region (Rajasthan) and the eastern region (Son valley) (Fig. 1A). The Supergroup overlies the Bundelkhand Granite massif (2.5 Ga; Azmi et al. 2008). The Semri Group occurs in the lower part of the Vindhyan succession and is primarily composed of carbonates and shales with subordinate sandstones and volcanoclastic units (Ramakrishnan and Vaidyanadhan 2008). The Upper Vindhyan succession comprises three groups, i.e., Kaimur, Rewa and Bhandar.

Vindhyan sequences were deposited mostly in shallow marine environments (Chanda and Bhattacharyya 1982). According to Bose et al. (1997, 2001), the Lower Vindhyan sedimentation occurred in an intracratonic rift basin, and the change from a rifted basin to an intracratonic sag basin occurred during the Upper Vindhyan deposition. Well preserved sections of the Semri and Kaimur Groups of the Vindhyan Supergroup are exposed in Son Valley, Central India.

The Semri Group is primarily characterised by its volcanogenic and biochemical sediments, whereas the overlying Kaimur Group is predominantly composed of siliciclastic deposits. The Kajrahat Limestone of the Semri Group is conformably underlain by the Basal Conglomerate and, in turn, is overlain by the Porcellanite Formation (Table 1). The Porcellanite Formation contains volcanic tuffs and rhyolite indicating significant felsic volcanic activity in the early Mesoproterozoic Era. The Kajrahat Limestone is exposed along the southern side of the Vindhyan basin in the Son Valley region (Rasmussen et al. 2002) (Fig. 1B).

The lower most and middle part of the Kajrahat Limestone Formation is exposed around Dala town and Kajrahat village, which is 1 km east of Dala town. The formation composed of alteration of thinly bedded and laminated limestones and characterized by the presence of stylolites along the stromatolitic layers. The upper division of this limestone formation consists of several shallowing-upward stromatolite cycles. The general trend is larger stromatolites are followed by smaller one at the top of the cycle (Banerjee et al. 2007). The middle part of the succession is characterized by Soft Sedimentary Deformation (SSD) structures. These are convolute bedding, contorted cross-bedding, autoclastic breccia, and small-scale folds characterized by narrow anticlines and broad synclines (Singh et al. 2020). The studied limestones are exposed in the vicinity of Dala town with a notable presence of different lithologies. The succession starts with thinly bedded grey coloured limestone which turns into laminated and then thickly bedded. After thickly bedded unit there is again alteration of laminated and thinly bedded unit (Fig. 2). In the study area three different facies

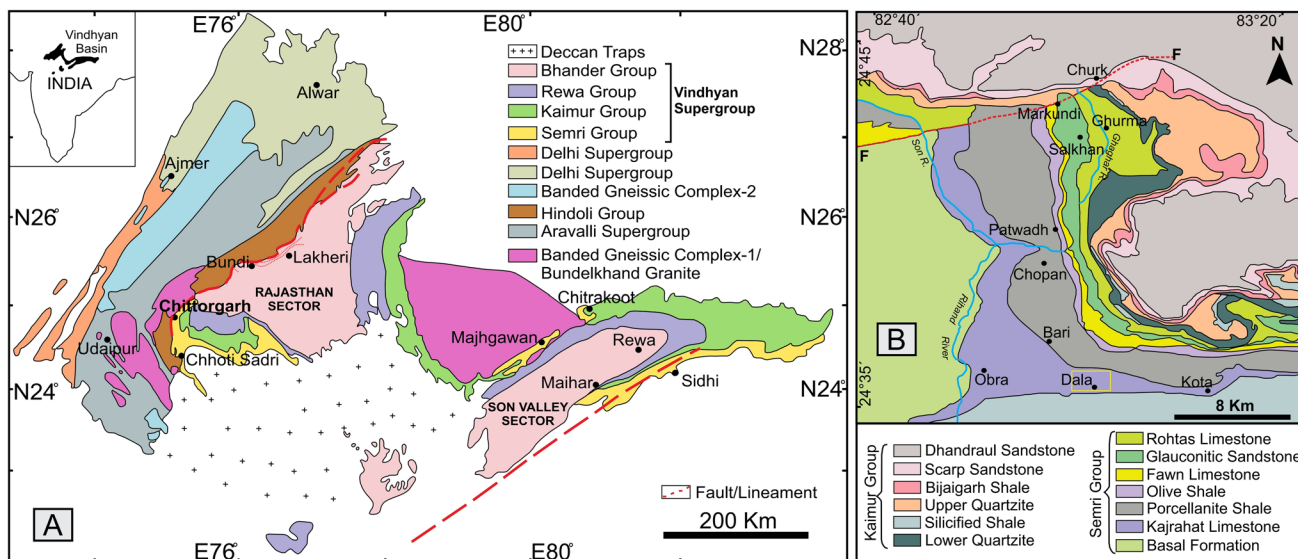


**Fig. 1** A Generalized geological map of the Vindhyan Supergroup, India (after Shukla et al. 2020). The samples of Kajrahat Limestone of Semri Group analyzed in the present study were collected

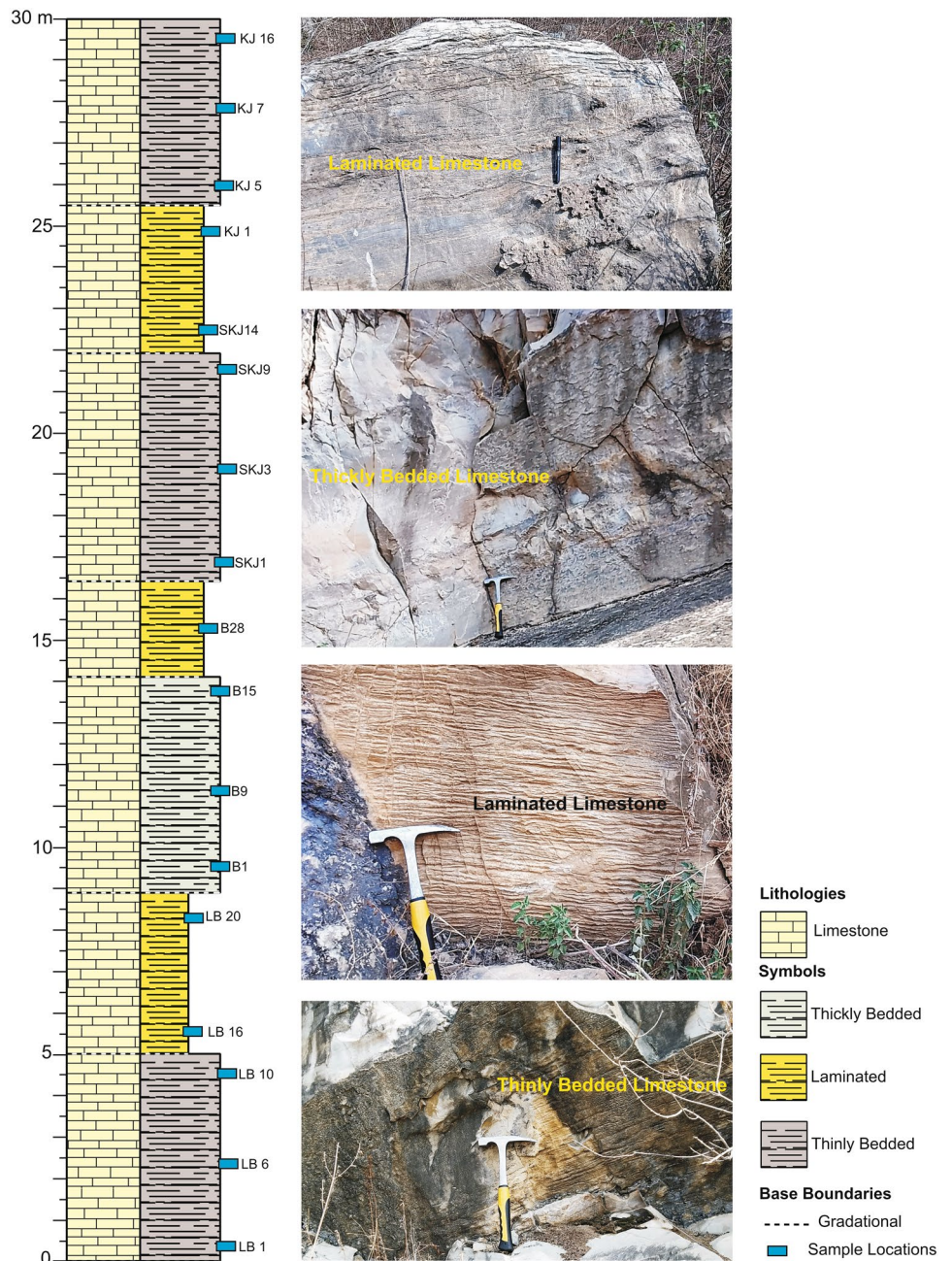
from nearby Dala Town. **B** Detailed geological map of the Vindhyan Supergroup in Son Valley (after Auden 1933). The yellow square represents the sampling area



**Table 1** Lithostratigraphic succession of Vindhyan Supergroup of Son valley, Central India (modified after Auden 1933; Kumar 1978)

		Kaimur Group	
		Unconformity	
Vindhyan Supergroup	Semri Group	Rohtas Limestone Formation	1599 ± 48 Ma (Sarangi et al. 2004)
		Kheinjua Formation	
		Chopan Porcellanite Formation	1631 ± 5 Ma (Rasmussen et al. 2002); 1628 ± 8 Ma (Ray et al. 2002); 1640 ± 4 Ma (Bickford et al. 2017)
		Kajrahat Limestone Formation	1600 ± 130 Ma (Ray et al. 2003)
		Basal Conglomerate Formation	

**Fig. 2** Litho-column displaying vertical organisation of different lithofacies in the Palaeoproterozoic Kajrahat Limestone with sample locations



are identified: laminated, thinly bedded and thickly bedded limestone. Gradational contacts are observed in between the different unit throughout the succession. Elephant skin weathering and stylolites are commonly found within these limestones.

## Methodology

Unweathered limestone samples were collected from the exposed outcrops of Kajrahat Limestone Formation, Vin-dhyan Basin located near Dala town. The selected samples were grinded in an agate mortar after washing with distilled water and subsequent air drying. The chemical analyses of seventeen representative samples were performed for major, trace and rare earth elements (REEs) at Wadia Institute of Himalayan Geology (WIHG), Dehradun, India. Sample preparation of major elements used pressed powder pellet mode and analyzed using X-Ray Fluorescence (XRF). The samples were dissolved using standard HF-HNO<sub>3</sub> dissolution technique for trace elements and REEs. About ~50 mg powdered samples were completely dissolved using ultra-pure acids. The final solutions were prepared in 2% HNO<sub>3</sub>. Then to avoid matrix effect highly diluted samples were analyzed using ICP-MS along with USGS rock standard BHVO-2.

## Results

### Major elements

Major element concentrations are listed in Table 2. The dominant oxide among all the oxide is CaO making up 30.87–48.59% (Table 2). CaO also shows a positive correlation with SiO<sub>2</sub> and TiO<sub>2</sub> (Table 4). On the other hand, MgO, shows variation ranging from 0.51 to 19.17%, (Table 2) and has a positive correlation with Fe<sub>2</sub>O<sub>3</sub>, MnO and Na<sub>2</sub>O (Table 4). The SiO<sub>2</sub> content ranges from 1.14 to 15.42% (Table 2) and shows negative correlation with Fe<sub>2</sub>O<sub>3</sub>, MgO, MnO, but positive correlation with TiO<sub>2</sub>, Al<sub>2</sub>O<sub>3</sub>, CaO, Na<sub>2</sub>O, K<sub>2</sub>O and P<sub>2</sub>O<sub>5</sub> (Table 4). Al<sub>2</sub>O<sub>3</sub> ranges from 0.23 to 4.09% (Table 2), and there is a negative correlation with CaO, MgO, and MnO (Table 4). In these limestones, the concentration of TiO<sub>2</sub> ranges from 0.02 to 0.11%. The amount of Fe<sub>2</sub>O<sub>3</sub> is relatively low ranging from 0.6 to 1.86% (Table 2). Additionally, Fe<sub>2</sub>O<sub>3</sub> and CaO have a negative correlation (Table 4). These limestones have very low concentrations of MnO (0.01–0.05), K<sub>2</sub>O (0.34–1.27), Na<sub>2</sub>O (0.02–0.05) and P<sub>2</sub>O<sub>5</sub> (0.12–0.78) (Table 2). The dolomitization ratio, as suggested by Singh et al. (2013) varies from 0.01 to 0.62 in the studied limestones. The PAAS-normalized major elements concentrations exhibit notable variations. The CaO content

is higher, while the Na<sub>2</sub>O content is moderately depleted in studied limestones (Fig. 3).

### Trace elements

The concentrations of trace elements are shown in Table 2. These trace elements are normalized using PAAS values (Taylor and McLennan 1985) and these values are important to know the minute enrichment and deficiencies in certain elements (Rollinson 1993). Additionally, their distribution is represented in the spider diagram (Fig. 4). The concentration of Cu and Sr shows large variations while the concentrations of other elements are relatively minimal (Table 2). As compared to PAAS, Ba and Co are significantly depleted, whereas Cu concentrations are roughly similar in some samples. The PAAS normalized patterns of studied limestones shows an enrichment in V, Sc, Cu, Zn, U and Sr while depletion in Ba, Co, Rb, Th, Zr (Fig. 5). The Sr concentrations in these limestones ranging from 126 to 514 ppm are lower than the average lithospheric carbonate value of 610 ppm. The Ba concentrations range from 10.1 to 38.4 ppm while U varies from 0.3 to 1.3 ppm (Table 2).

### Rare earth elements

The concentrations of REEs are reported in Table 2 and are normalized to PAAS values (Taylor and McLennan 1985) in Fig. 5. The limestones show seawater like REE pattern with negative Ce and Eu anomaly (except for three samples which shows positive Eu anomaly). The ΣREE content varies significantly among the limestone samples, ranging from 13.7 to 68.3 ppm. The LREE ranges from 13 to 64.2 ppm, while the HRRE ranges from 0.7 to 4.1 ppm. The higher content of REE than typical marine carbonate indicates the presence of silt and clay fractions because REE accommodated easily in the clay structure (McLennan 1989). The ΣREE shows a positive correlation with SiO<sub>2</sub>, TiO<sub>2</sub>, Al<sub>2</sub>O<sub>3</sub> ( $r^2 = 0.87, 0.84, 0.91$ , respectively) and a weak positive correlation with CaO ( $r^2 = 0.12$ ) (Table 4). Correlation pattern indicates that the concentration of these elements may control by the influence of terrigenous material. The PASS-normalized REE patterns of these limestones (Fig. 5) exhibit a minor enrichment in LREE relative to HREE. Additionally, these samples exhibit a negative Ce anomaly ( $Ce/Ce^* = 0.66–0.89$ ) (Table 3). Similarly, most of the studied samples show negative Eu anomalies ( $Eu/Eu^* = 0.88–0.94$ ), barring three samples ( $Eu/Eu^* = KJ5 = 1.07, KJ1 = 1.09, LB10 = 1.43$ ; Table 3). The majority of the samples show positive La anomalies, negative Ce anomalies, positive Gd anomalies and negative Eu anomalies (Fig. 5). The  $(Gd/Yb)_N$  ratio varies from 1.53 to 2.33 with an average of 1.81, whereas the  $(La/Yb)_N$  ratio varies from 0.98 to 2.13 (Table 3) with an average value of 1.48.

**Table 2** Major (wt %), trace and rare earth elements concentrations (ppm) for the Kajrahat Limestone of Vindhyan basin, Central India

Sample	KJ16	KJ7	KJ5	KJ1	SKJ14	SKJ9	SKJ3	SKJ1	B28	B15	B9	B1	LB20	LB16	LB10	LB6	LB1
SiO <sub>2</sub>	7.28	14.97	8.80	14.35	12.55	12.54	11.21	11.37	13.19	12.95	9.48	9.51	15.42	12.08	1.14	9.22	10.27
TiO <sub>2</sub>	0.05	0.11	0.05	0.08	0.09	0.08	0.08	0.07	0.10	0.11	0.08	0.08	0.13	0.08	0.02	0.10	0.08
Al <sub>2</sub> O <sub>3</sub>	1.09	2.76	1.24	2.41	2.47	2.35	2.19	2.24	2.79	2.94	2.10	1.80	4.09	2.40	0.23	1.89	2.49
Fe <sub>2</sub> O <sub>3</sub>	0.88	0.89	0.74	1.36	1.23	0.95	1.29	1.24	1.47	1.65	1.11	1.46	1.35	1.45	1.86	0.60	1.03
MnO	0.01	0.01	0.01	0.03	0.02	0.01	0.02	0.02	0.01	0.01	0.01	0.01	0.02	0.01	0.05	0.01	0.01
CaO	46.56	43.78	48.59	44.08	41.85	44.63	42.37	41.94	39.89	40.54	43.93	41.89	37.2	39.88	30.87	46.70	42.26
MgO	2.39	0.87	0.51	0.71	3.28	1.07	3.35	3.16	4.32	3.84	2.94	4.36	4.96	4.99	19.17	0.80	3.31
Na <sub>2</sub> O	0.02	0.03	0.02	0.03	0.03	0.03	0.03	0.03	0.04	0.04	0.03	0.03	0.05	0.03	0.02	0.02	0.03
K <sub>2</sub> O	0.39	0.64	0.34	0.60	0.65	0.58	0.58	0.57	0.81	0.86	0.7	0.68	1.27	0.81	0.14	0.64	0.79
P <sub>2</sub> O <sub>5</sub>	0.16	0.41	0.12	0.44	0.37	0.19	0.25	0.23	0.50	0.66	0.78	0.38	0.60	0.43	0.03	0.35	0.45
SUM	58.83	64.46	60.41	64.09	62.55	62.43	61.37	60.87	63.12	63.6	61.16	60.19	65.08	62.16	53.54	60.32	60.73
LOI	39.81	35.15	38.67	36.07	37.40	36.80	38.00	42.78	36.94	36.84	38.77	39.04	35.54	37.79	45.72	38.00	37.43
D.R	0.05	0.02	0.01	0.02	0.08	0.02	0.08	0.07	0.11	0.09	0.07	0.10	0.13	0.12	0.62	0.02	0.08
Ba	23.90	30.90	21.10	32.60	31.20	30.90	27.40	28.70	15.50	38.40	13.50	34.80	11.60	31.10	10.10	30.50	32.10
V	19.60	23.60	19.60	22.50	24.50	25.30	22.60	23.90	20.30	28.90	20.20	19.60	35.70	28.40	18.70	28.00	29.40
Sc	2.80	3.80	3.20	3.20	3.40	3.00	2.80	2.80	3.30	4.10	3.30	3.20	5.10	3.60	2.10	3.90	3.90
Co	1.60	2.50	2.60	2.70	2.30	2.40	2.00	2.30	2.50	3.00	2.70	2.20	3.40	2.50	1.60	2.90	2.20
Cu	16.10	53.40	33.50	31.80	9.50	9.40	6.60	6.90	4.20	9.20	3.60	3.60	12.30	9.80	8.60	11.90	8.40
Rb	15.40	27.40	13.90	23.90	27.70	24.10	21.40	23.50	30.00	36.30	26.30	24.30	57.70	31.40	4.30	29.80	32.60
Zn	18.10	21.70	17.70	21.10	23.90	18.30	15.90	17.10	25.10	47.9	18.80	34.00	31.60	24.50	14.30	22.60	20.40
Pb	4.40	5.40	4.70	6.10	4.90	4.90	4.40	4.60	5.50	5.70	4.40	5.60	6.00	4.70	3.50	5.80	4.80
Th	1.40	3.10	1.40	2.20	2.40	2.60	2.10	2.40	3.20	3.10	2.30	2.20	4.20	2.20	0.40	2.70	2.30
U	0.30	0.80	0.40	0.40	0.40	0.60	0.30	0.40	0.60	0.50	1.30	0.50	0.50	0.30	0.50	0.60	0.60
Zr	16.40	35.40	18.60	21.80	24.60	24.90	18.00	21.70	28.60	34.60	21.70	20.70	41.40	25.70	4.40	34.80	33.10
Sr	137.0	139.0	134.0	134.0	154.0	144.0	144.0	145.0	316.0	347.0	426.0	240.0	145.0	126.0	480.0	514.0	417.0
La	6.66	9.90	7.42	8.83	8.46	9.23	7.05	8.41	8.75	9.34	8.11	6.68	14.68	8.89	2.48	8.77	8.85
Ce	12.38	20.95	14.66	17.11	15.51	18.50	14.79	15.62	17.94	18.18	15.21	13.25	28.24	18.12	5.61	15.24	16.07
Pr	1.57	2.80	2.12	2.40	1.93	2.37	1.87	1.91	2.38	2.38	2.03	1.78	3.59	2.46	0.88	1.90	2.07
Nd	4.84	9.75	7.93	8.42	6.13	7.59	6.06	6.74	8.26	8.16	6.73	6.04	12.65	8.86	2.92	5.92	6.51
Sm	0.87	1.97	1.59	1.59	1.12	1.42	1.12	1.12	1.55	1.56	1.24	1.16	2.35	1.67	0.51	1.10	1.20
Eu	0.17	0.36	0.37	0.37	0.20	0.24	0.20	0.23	0.29	0.30	0.26	0.21	0.42	0.31	0.15	0.20	0.23
Gd	0.79	1.86	1.64	1.59	1.01	1.26	1.00	1.17	1.43	1.51	1.19	1.10	2.26	1.57	0.47	1.03	1.11
Tb	0.10	0.27	0.25	0.23	0.13	0.18	0.13	0.14	0.19	0.21	0.16	0.15	0.32	0.21	0.06	0.14	0.15
Dy	0.53	1.47	1.40	1.19	0.68	0.90	0.67	0.77	1.02	1.10	0.83	0.81	1.65	1.11	0.29	0.76	0.76
Ho	0.11	0.30	0.28	0.23	0.13	0.18	0.13	0.17	0.21	0.22	0.17	0.16	0.33	0.22	0.06	0.15	0.15
Er	0.28	0.77	0.73	0.61	0.36	0.49	0.35	0.39	0.55	0.6	0.45	0.44	0.88	0.57	0.15	0.43	0.40
Tm	0.04	0.11	0.10	0.08	0.05	0.07	0.05	0.05	0.08	0.09	0.06	0.07	0.13	0.08	0.02	0.06	0.06
Yb	0.23	0.68	0.56	0.49	0.33	0.42	0.31	0.37	0.51	0.54	0.39	0.41	0.78	0.49	0.12	0.40	0.39
Lu	0.04	0.10	0.10	0.08	0.05	0.07	0.05	0.05	0.08	0.09	0.06	0.07	0.13	0.08	0.02	0.06	0.06
ΣREE	28.60	51.20	39.00	43.10	36.00	42.80	33.70	37.10	43.20	44.20	36.80	32.30	68.30	44.60	13.70	36.10	37.90
LREE	27.30	47.60	35.70	40.30	34.40	40.60	32.10	35.20	40.60	41.40	34.80	30.20	64.20	41.90	13.00	34.20	36.00
HREE	1.30	3.60	3.30	2.80	1.60	2.20	1.60	1.90	2.60	2.80	2.00	2.10	4.10	2.70	0.70	1.90	1.90
LREE/HREE	21.00	13.22	10.82	14.39	21.50	18.45	20.06	18.53	15.62	14.79	17.40	14.38	15.66	15.52	18.57	18.00	18.95

## Discussion

### Significance of major and trace elements

The studied limestones contain a significant amount of CaO

(Table 2). The primary carbonate phase is mainly calcite, as indicated by the high concentration of CaO and the low percentage of MgO, which is further supported by the minimal dolomitization ratio. The concentration of SiO<sub>2</sub> varies from 1.14 to 14.97%. The relatively higher concentration



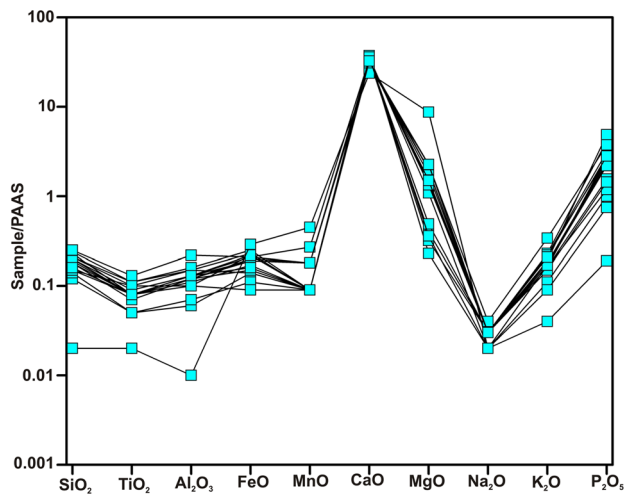


**Fig. 3** Plot of Post-Archean Australian Shale normalized major elements pattern of Kajrahat Limestone

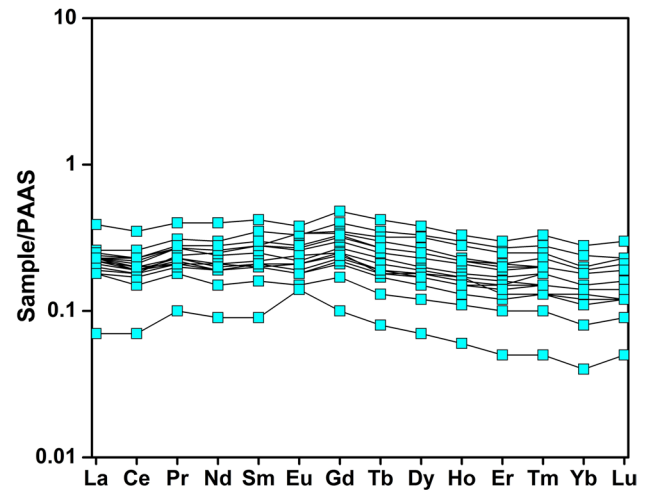


**Fig. 5** Plot of Post-Archean Australian Shale normalized rare earth elements pattern of Kajrahat Limestone

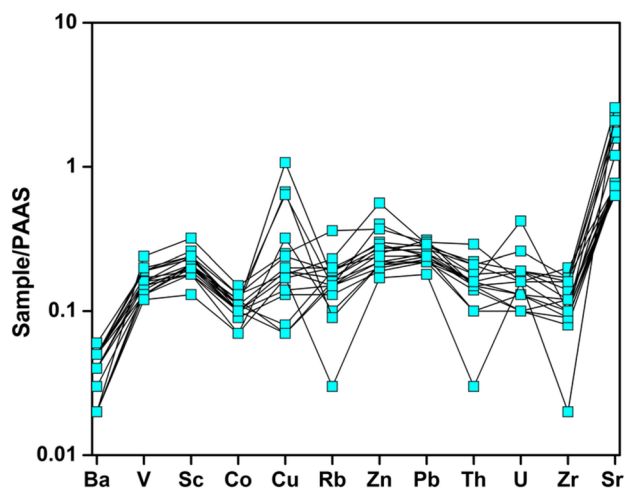


**Fig. 4** Plot of Post-Archean Australian Shale normalized trace elements pattern of Kajrahat Limestone

of  $\text{SiO}_2$  may be due to the more continental influx during the deposition of the limestone in shallow marine condition. The low concentrations of other oxides such as  $\text{TiO}_2$ ,  $\text{Al}_2\text{O}_3$ ,  $\text{Fe}_2\text{O}_3$ ,  $\text{MnO}$ ,  $\text{Na}_2\text{O}$ ,  $\text{K}_2\text{O}$ , and  $\text{P}_2\text{O}_5$  (Table 2) and their positive correlation with  $\text{SiO}_2$  indicates that these oxides are associated with a siliciclastic phase that was present in the examined limestones as impurities/detrital admixtures. Primarily Ca is biogenic in origin and in spite of its original distribution is basically behaved as a dilutant for all other constituents. This is evident by its negative correlations with most of the major and trace elements (Table 4). The relation between  $\text{Al}_2\text{O}_3$  and  $\text{Fe}_2\text{O}_3$  differentiates between inland and marine limestones by the negative and positive correlation, respectively (Zhang et al. 2017). The studied samples show positive relation between these two oxides (Table 4) which

indicate its marine nature. In contrast,  $\text{Al}_2\text{O}_3$  has a negative correlation with  $\text{MnO}$  for all the limestones ( $r^2 = -0.37$ ), which indicates that the concentration of  $\text{MnO}$  is may not be controlled by clay minerals but other input to the limestone geochemistry has a significant role. The  $\text{P}_2\text{O}_5$  contents are well correlated with  $\text{TiO}_2$  ( $r^2 = 0.72$ ),  $\text{Fe}_2\text{O}_3$  ( $r^2 = 0.16$ ) and  $\text{K}_2\text{O}$  ( $r^2 = 0.78$ ) (Table 4), implying that some, maybe most, of the  $\text{P}_2\text{O}_5$  contents in these limestones may not be biogenic, because  $\text{TiO}_2$  and  $\text{K}_2\text{O}$  are principally derived from aluminosilicate clastics and  $\text{Fe}_2\text{O}_3$  from hydrothermal Fe–Mn-oxhydroxides (e.g., Murray 1994). All of the major oxides except CaO, MnO, MgO showing positive correlation with each other. So, the geochemical pattern of major oxides reveals that the geochemistry of the present studied limestones is basically managed by the tectonic environment of the basin that may be volcanic activity, topographic elevation and the distance away from the continent.

The trace elements of the studied limestones viewed by their positive correlation with  $\text{Al}_2\text{O}_3$ ,  $\text{TiO}_2$  (Table 4), which indicates that their concentrations primarily controlled by detrital siliciclastic fractions. The concentrations of the high-strength-field elements (HSFES; e.g., Th, U, Sc, Zr) and the transitional trace elements (e.g., Co, Cu), in the studied limestones are generally lower by one order of magnitude when compared to the PAAS (Fig. 4). However, the contents of the large-ion-lithophile elements (LILEs; e.g. Ba, Rb, Sr) in these limestones exhibit large range. The studied limestones reveal that Sr is the most abundant trace element in them. The Sr concentration in sedimentary rocks varies due to various factors that affect Sr in depositional environments under low temperatures. The presence of Ca can make an impact on the distribution of Sr, causing additional Sr to be incorporated into diagenetic carbonate. Additionally, weathering of feldspars, specifically plagioclase can result in

**Table 3** Elemental ratios in the Kajrahat Limestone of Vindhyan basin, Central India

Sample	KJ16	KJ7	KJ5	KJ1	SKJ14	SKJ9	SKJ3	SKJ1	B28	B15	B9	B1	LB20	LB16	LB10	LB6	LB1
La/Sc	2.38	2.61	2.32	2.76	2.49	3.08	2.52	3.00	2.65	2.28	2.46	2.09	2.88	2.47	1.18	2.25	2.27
La/Co	4.16	3.96	2.85	3.27	3.68	3.85	3.53	3.66	3.50	3.11	3.00	3.04	4.32	3.56	1.55	3.02	4.02
Th/Sc	0.50	0.82	0.44	0.69	0.71	0.87	0.75	0.86	0.97	0.76	0.70	0.69	0.82	0.61	0.19	0.69	0.59
Th/Co	0.88	1.24	0.54	0.81	1.04	1.08	1.05	1.04	1.28	1.03	0.85	1.00	1.24	0.88	0.25	0.93	1.05
U/Th	0.21	0.26	0.29	0.18	0.17	0.23	0.14	0.17	0.19	0.16	0.57	0.23	0.12	0.14	1.25	0.22	0.26
La/Th	4.76	3.19	5.30	4.01	3.53	3.55	3.36	3.50	2.73	3.01	3.53	3.04	3.50	4.04	6.20	3.25	3.85
Er/Nd	0.06	0.08	0.09	0.07	0.06	0.06	0.06	0.06	0.07	0.07	0.07	0.07	0.07	0.06	0.05	0.07	0.06
(La/Yb) <sub>N</sub>	2.13	1.07	0.98	1.33	1.89	1.62	1.68	1.67	1.26	1.27	1.53	1.20	1.39	1.34	1.52	1.62	1.67
(La/Nd) <sub>N</sub>	1.16	0.86	0.79	0.88	1.16	1.02	0.98	1.05	0.89	0.96	1.01	0.93	0.98	0.84	0.72	1.25	1.14
(Gd/Yb) <sub>N</sub>	2.05	1.63	1.74	1.93	1.82	1.79	1.92	1.88	1.67	1.67	1.82	1.60	1.73	1.91	2.33	1.53	1.70
(Pr/Yb) <sub>N</sub>	2.15	1.30	1.19	1.54	1.84	1.78	1.90	1.62	1.47	1.39	1.64	1.37	1.45	1.58	2.31	1.49	1.67
(Nd/Yb) <sub>N</sub>	1.84	1.25	1.24	1.50	1.63	1.58	1.71	1.59	1.42	1.32	1.51	1.29	1.42	1.58	2.13	1.30	1.46
(Dy/Yb) <sub>N</sub>	1.47	1.38	1.59	1.55	1.31	1.36	1.38	1.32	1.27	1.30	1.35	1.26	1.35	1.44	1.54	1.21	1.24
Eu/Eu*	0.96	0.88	1.07	1.09	0.88	0.84	0.88	0.94	0.91	0.91	1.00	0.87	0.85	0.89	1.43	0.88	0.93
Ce/Ce*	0.77	0.81	0.80	0.77	0.80	0.78	0.80	0.89	0.81	0.81	0.77	0.78	0.86	0.82	0.66	0.79	0.77
Pr/Pr*	1.15	1.11	1.12	1.14	1.13	1.14	1.12	1.06	1.11	1.11	1.14	1.13	1.08	1.10	1.24	1.14	1.15

Sr fractionation (Fairbridge 1972). The negative correlation between Sr and CaO (Table 4) indicates that the Sr and CaO are not genetically connected. Therefore, the enrichment of Sr content may be attributed either from its own minerals or from the siliciclastic materials. The presence of appreciable amount of trace elements like Ba, V, Cu, Rb, Zn, and Zr suggests that either these elements have replaced certain cations or they have formed their own minerals in small quantities. The weak positive and negative correlations of these trace elements with CaO (Table 4), indicate that they are either present in their own minerals or because of the siliciclastic input. Additionally, the presence of siliciclastic impurities in limestone may be responsible for the presence of feldspars and mica, resulting in to the presence of barium. Reeder (1983) suggested that under specific conditions, certain divalent cations like Pb, Cu, Co, Ni and others can substitute for Ca in calcite. This suggests that during the deposition of limestone, Ca may have replaced by Pb, Ni, Co and Cu under appropriate conditions. The Mn-Sr correlation is useful for determining diagenetic changes in limestones (Brand and Veizer 1980). However, there is no significant correlation between Mn and Sr in this study ( $r^2=0.14$ ). This indicates that the studied limestones have not experienced major diagenetic changes and may still preserve their original geochemical fingerprints.

### Significance of uranium in the marine environment

The redox conditions in seawater influence uranium, causing uranium ions to remain in a higher oxidation state ( $U^{6+}$ ) in an oxidizing environment. This leads to the formation of a soluble compound called uranyl tricarbonate [ $UO_2$

( $CO_3$ )<sub>3</sub><sup>4-</sup>]. They maintain a lower oxidation state ( $U^{4+}$ ) under reducing circumstances, and forming insoluble uranous fluoride that becomes immobilized within marine carbonates (Wignall and Twitchett 1996). Uranium is mobile in aqueous solutions, whereas Th is generally immobile (Anderson et al. 1983; Nozaki et al. 1981; Wright et al. 1984). Within continental margin settings, uranium can undergo fractionation similarly to Ce, leading to its separation from other rare earth elements (REEs) (Whittaker and Kyser 1993). In the studied limestones, the U concentration is relatively low, ranging from 0.3 to 1.3 (Table 5). This contrasts with sediments originating from the oxygen minimum zone (Nath et al. 1997). However, the U concentrations in the studied limestones are comparable to those observed in shallow-marine carbonates and the Kudankulam Limestone which were deposited under oxygen-rich conditions (Madhavaraju and Ramasamy 1999; Table 5). This shows that the studied limestones with a low U concentration are affected by the oxygenation level in the water column. In an oxygen-rich conditions (oxic environment), U is readily leached from the sediments and transferred into the water column. Conversely, under reducing conditions, U is extracted from seawater and precipitates onto the sediments. In some instances, there is no significant reduction of  $U^{6+}$  to  $U^{4+}$  observed in anoxic and suboxic environments (Anderson et al. 1989). In this particular case, sedimentary geochemists attempted to use the U/Th ratio as a redox indicator rather than the U concentration (Wright et al. 1984; Jones and Manning 1994). K and Th are present in the detrital clay fraction of marine mudrocks shows close correlation (Myers and Wignall 1987). U also present in the detrital clay fraction but behaves differently than Th, it is also transfer to some extent



**Table 4** Inter elemental relationship among the major oxides, trace and rare earth elements in the Kajrahat Limestone

	SiO <sub>2</sub>	TiO <sub>2</sub>	Al <sub>2</sub> O <sub>3</sub>	Fe <sub>2</sub> O <sub>3</sub>	MnO	CaO	MgO	Na <sub>2</sub> O	K <sub>2</sub> O	P <sub>2</sub> O <sub>5</sub>	Ba	V	Sc	Co	Cu	Rb	Zn	Pb	
SiO <sub>2</sub>	1.00																		
TiO <sub>2</sub>	0.85	1.00																	
Al <sub>2</sub> O <sub>3</sub>	0.91	0.93	1.00																
Fe <sub>2</sub> O <sub>3</sub>	-0.11	-0.08	0.04	1.00															
MnO	-0.45	-0.47	-0.37	0.56	1.00														
CaO	0.24	0.09	-0.02	-0.85	-0.68	1.00													
MgO	-0.66	-0.49	-0.44	0.70	0.76	-0.88	1.00												
Na <sub>2</sub> O	0.71	0.77	0.89	0.41	-0.15	-0.35	-0.09	1.00											
K <sub>2</sub> O	0.74	0.88	0.93	0.11	-0.40	-0.11	-0.31	0.88	1.00										
P <sub>2</sub> O <sub>5</sub>	0.56	0.72	0.70	0.16	-0.38	-0.03	-0.28	0.68	0.78	1.00									
Ba	0.36	0.24	0.17	-0.16	-0.39	0.41	-0.50	-0.08	0.07	0.03	1.00								
V	0.53	0.68	0.74	-0.03	-0.19	-0.14	-0.17	0.59	0.78	0.43	0.19	1.00							
Sc	0.65	0.85	0.81	-0.15	-0.43	0.06	-0.37	0.66	0.88	0.67	0.11	0.84	1.00						
Co	0.66	0.78	0.74	-0.11	-0.33	0.13	-0.42	0.62	0.74	0.68	0.04	0.65	0.83	1.00					
Cu	0.27	0.08	0.02	-0.40	-0.03	0.36	-0.33	-0.19	-0.19	-0.14	0.14	-0.09	0.13	0.13	1.00				
Rb	0.73	0.89	0.93	0.03	-0.37	-0.09	-0.31	0.84	0.98	0.72	0.07	0.86	0.93	0.79	-0.11	1.00			
Zn	0.40	0.61	0.52	0.37	-0.31	-0.15	-0.10	0.61	0.61	0.59	0.36	0.44	0.61	0.55	-0.15	0.59	1.00		
Pb	0.73	0.79	0.69	-0.10	-0.35	0.24	-0.53	0.54	0.66	0.52	0.37	0.47	0.71	0.75	0.24	0.68	0.63	1.00	
Th	0.85	0.97	0.95	-0.07	-0.46	0.05	-0.47	0.83	0.90	0.68	0.13	0.69	0.83	0.78	0.02	0.91	0.55	0.76	
U	0.02	0.21	0.12	-0.18	-0.22	0.07	-0.08	0.10	0.15	0.56	-0.30	-0.10	0.16	0.27	0.01	0.12	-0.03	0.00	
Zr	0.75	0.92	0.85	-0.26	-0.55	0.17	-0.51	0.63	0.84	0.64	0.27	0.79	0.93	0.77	0.16	0.88	0.55	0.74	
Sr	-0.51	-0.10	-0.27	0.10	0.14	-0.27	0.41	-0.18	-0.09	0.21	-0.22	-0.02	0.00	0.00	-0.38	-0.08	0.08	-0.12	
La	0.85	0.87	0.92	-0.22	-0.44	0.16	-0.54	0.75	0.88	0.59	0.09	0.78	0.88	0.81	0.16	0.92	0.41	0.70	
Ce	0.88	0.86	0.93	-0.15	-0.42	0.11	-0.50	0.78	0.86	0.57	0.07	0.73	0.84	0.78	0.23	0.89	0.41	0.68	
Pr	0.87	0.82	0.90	-0.12	-0.39	0.10	-0.48	0.76	0.82	0.57	0.04	0.68	0.82	0.80	0.31	0.84	0.41	0.68	
Nd	0.84	0.76	0.85	-0.06	-0.34	0.07	-0.43	0.74	0.77	0.53	0.00	0.62	0.78	0.80	0.36	0.79	0.40	0.66	
Sm	0.82	0.74	0.81	-0.09	-0.37	0.10	-0.45	0.69	0.73	0.51	0.02	0.57	0.77	0.78	0.43	0.74	0.41	0.66	
Eu	0.68	0.53	0.62	-0.05	-0.20	0.11	-0.37	0.54	0.53	0.43	-0.07	0.39	0.63	0.74	0.55	0.55	0.30	0.58	
Gd	0.79	0.70	0.77	-0.09	-0.34	0.12	-0.45	0.66	0.69	0.50	0.01	0.54	0.75	0.80	0.46	0.71	0.40	0.66	
Tb	0.75	0.65	0.71	-0.13	-0.32	0.16	-0.44	0.59	0.62	0.45	0.01	0.49	0.73	0.78	0.53	0.65	0.38	0.65	
Dy	0.73	0.63	0.67	-0.16	-0.35	0.20	-0.46	0.55	0.58	0.42	0.02	0.45	0.70	0.77	0.56	0.61	0.37	0.64	
Ho	0.72	0.62	0.67	-0.17	-0.35	0.19	-0.46	0.55	0.57	0.41	0.00	0.43	0.69	0.76	0.56	0.60	0.35	0.62	
Er	0.73	0.66	0.68	-0.17	-0.37	0.20	-0.47	0.57	0.60	0.45	0.02	0.46	0.73	0.80	0.54	0.63	0.40	0.67	
Tm	0.72	0.70	0.71	-0.14	-0.40	0.16	-0.44	0.61	0.66	0.47	0.04	0.50	0.77	0.79	0.48	0.68	0.48	0.69	
Yb	0.78	0.76	0.78	-0.14	-0.42	0.15	-0.47	0.65	0.71	0.52	0.05	0.54	0.80	0.82	0.46	0.73	0.47	0.72	
Lu	0.72	0.69	0.72	-0.12	-0.40	0.15	-0.44	0.63	0.68	0.48	0.02	0.52	0.78	0.81	0.43	0.70	0.50	0.70	

Table 4 (continued)

	SiO <sub>2</sub>	TiO <sub>2</sub>	Al <sub>2</sub> O <sub>3</sub>	Fe <sub>2</sub> O <sub>3</sub>	MnO	CaO	MgO	Na <sub>2</sub> O	K <sub>2</sub> O	P <sub>2</sub> O <sub>5</sub>	Ba	Tb	Dy	Ho	Er	Tm	Yb	Zn	Pb
ΣREE	0.87	0.84	0.91	-0.14	-0.41	0.12	-0.50	0.76	0.83	0.57	0.05	0.70	0.84	0.81	0.29	0.86	0.42	0.69	ΣREE
Th		U	Zr	Sr	La	Ce	Pr	Nd	Sm	Eu	Gd	Tb	Dy	Ho	Er	Tm	Yb	Zn	Pb
SiO <sub>2</sub>	0.87																		
TiO <sub>2</sub>		0.84																	
Al <sub>2</sub> O <sub>3</sub>			0.91																
Fe <sub>2</sub> O <sub>3</sub>				-0.14															
MnO					-0.41														
CaO						0.12													
MgO							-0.50												
Na <sub>2</sub> O								0.76											
K <sub>2</sub> O									0.83										
P <sub>2</sub> O <sub>5</sub>										0.57									
Ba											0.05								
V													0.70						
Sc														0.84					
Co															0.81				
Cu																0.29			
Rb																	0.86		
Zn																		0.42	
Pb																			0.69
Th	1.00																		
U	0.21	1.00																	
Zr	0.91	0.20	1.00																
Sr	-0.15	0.49	0.01	1.00															
La	0.91	0.11	0.88	-0.32	1.00														
Ce	0.91	0.10	0.85	-0.40	0.98	1.00													
Pr	0.86	0.11	0.81	-0.41	0.95	0.99	1.00												
Nd	0.81	0.08	0.74	-0.44	0.90	0.95	0.99	1.00											
Sm	0.77	0.10	0.73	-0.44	0.87	0.93	0.97	0.99	1.00										
Eu	0.56	0.09	0.54	-0.40	0.70	0.76	0.85	0.91	0.93	1.00									
Gd	0.73	0.08	0.70	-0.44	0.84	0.90	0.95	0.98	0.99	0.96	1.00								
Tb	0.68	0.09	0.66	-0.42	0.80	0.86	0.92	0.96	0.98	0.97	0.99	1.00							
Dy	0.65	0.08	0.65	-0.43	0.77	0.83	0.90	0.94	0.97	0.97	0.99	1.00	1.00						
Ho	0.66	0.10	0.64	-0.43	0.77	0.83	0.90	0.94	0.96	0.96	0.98	0.99	1.00	1.00					
Er	0.68	0.11	0.68	-0.39	0.79	0.84	0.91	0.94	0.97	0.96	0.98	0.99	1.00	0.99	1.00				

Table 4 (continued)

	Th	U	Zr	Sr	La	Ce	Pr	Nd	Sm	Eu	Gd	Tb	Dy	Ho	Er	Tm	Yb	Lu	$\Sigma$ REE
Tm	0.72	0.10	0.71	-0.36	0.80	0.85	0.91	0.94	0.97	0.93	0.97	0.98	0.98	0.98	0.99	1.00			
Yb	0.79	0.15	0.78	-0.33	0.84	0.89	0.94	0.96	0.98	0.92	0.98	0.98	0.98	0.98	0.98	0.99	1.00		
Lu	0.72	0.08	0.71	-0.36	0.81	0.86	0.91	0.94	0.97	0.93	0.97	0.98	0.98	0.97	0.99	1.00	0.98	1.00	
$\Sigma$ REE	0.88	0.10	0.83	-0.40	0.97	0.99	1.00	0.98	0.96	0.83	0.94	0.91	0.89	0.89	0.90	0.90	0.94	0.91	1.00

in solution as uranyl carbonate complexes (Langmuir 1978). The reducing conditions are favorable for its precipitation which tends to enrich the sediment in authigenic (nondetrital) uranium. The authigenic component of U can be calculated if detrital component is known. The U is assumed to be purely detrital, is 3 in the normal mudstone with minimum Th/U ratio. The concentration of U which is associated with the detrital fraction can thus be estimated by dividing the measured Th content by 3. Authigenic U in the sample is the difference between the actual U measured and the calculated detrital U. Reducing conditions and the presence of a sorbent, which is usually organic matter or phosphate, favoured the presence of U at the sediment–water interface (Kochenov et al. 1977; Holland 1984). Therefore, sediments enriched in authigenic U indicate anoxic depositional conditions that allow both large amounts of organic matter to accumulate and U to be fixed. Ratios of U/Th exceeding 1.25 are indicators of suboxic and anoxic conditions and have been utilized to infer such environments. Additionally, sediments from the Arabian Sea in the oxygen minimum zone exhibit a notably high U/Th ratio (> 1.25) (Nath et al. 1997). The studied limestones exhibit a U/Th ratio (0.12–1.25, Table 3) which is lower than the samples deposited under anoxic and suboxic conditions. Nevertheless, the U/Th in these limestones is similar to shallow-marine carbonates found in southern India that were deposited under an oxic environment (Madhavaraju and Ramasamy 1999; Table 5). This strongly shows that the studied limestone was also deposited under oxic conditions. Moreover, the studied limestone samples show minimal variations in both U contents and U/Th ratios. This suggests that there were no significant changes in oxygen levels within the water column during deposition of these shallow-marine limestones.

### Source of REE and provenance characteristics

Total REE abundances ( $\Sigma$ REE) of the studied limestones are generally lower when compared to the PAAS. The  $\Sigma$ REE concentrations in studied limestone samples ranging from 13.7 to 68.3 are comparable to Upper Cretaceous shallow-marine carbonates (Madhavaraju and Ramasamy 1999) and modern Arabian Sea carbonates (Nath et al. 1997) (Table 5). The variation in the  $\Sigma$ REE content among different samples is primarily due to differences in the terrigenous sediment content within the limestone samples. This is likely attributed to lower levels of Si and Al and higher  $\text{CaCO}_3$  content, suggesting that the  $\Sigma$ REE content is influenced by impurities other than carbonate.

The low  $\Sigma$ REE in certain samples of studied limestones is attributed to the presence of marine carbonate phases. These phases typically have lower rare earth elements (REEs) compared to detrital clays and heavy minerals (Piper 1974; Palmer 1985). In limestone samples, the REE contents are

**Table 5** Comparison of the average values of the studied Kajrahat Limestone to the shallow and deep water marine carbonate sediments

Elements ratios	Kajrahat Limestone <sup>o</sup>	Kudankulam Limestone <sup>a</sup>	Shallow marine carbonate <sup>b</sup>	Shallow marine platform carbonate <sup>c</sup>	Arabian Sea Carbonate sediments <sup>d</sup>	Indian Ocean Carbonate Sediments <sup>e</sup>	Shahabad Formation Limestone			Sea water	
							Grey Limestone <sup>f</sup> (GL)	Yellowish Limestone <sup>f</sup> (YL)	Brown Limestone <sup>f</sup> (BL)		
Ce/Ce*	0.66–0.89	0.90±0.06	0.76±0.16	–	0.84±0.06	0.30–0.84 Avg. 0.56	0.35–0.63 (0.54±0.1)	0.50–0.64 (0.57±0.05)	0.58–0.66 (0.62±0.12)	0.57±0.08	<0.1–0.4 <sup>g</sup>
(La/Yb) <sub>N</sub>	0.98–2.13	2.69±1.37	1.82±0.46	0.68±0.47	0.85±0.2	0.166±0.953	0.52–0.84 (0.73±0.12)	0.48–0.89 (0.71±0.15)	0.59–0.86 (0.77±0.12)	0.732±0.12	0.2–0.5 <sup>h</sup>
(La/Nd) <sub>N</sub>	0.72–1.25	1.17±0.09	1.22±0.26	1.01±0.20	0.98±0.03	1.04±0.19	0.84– 1.35(1.09±0.19)	0.99–1.33 (1.15±0.14)	1.09–1.20 (1.23±0.24)	1.15±0.19	0.8–2.0 <sup>i</sup>
(Nd/Yb) <sub>N</sub>	1.24–2.13	2.29±1.17	1.51±0.30	0.65±0.39	0.85±0.17	0.83±0.13	0.60–0.74 (0.67±0.05)	0.48–0.72 (0.42±0.09)	0.53–0.76 (0.61±0.11)	0.64±0.08	0.205–0.497 <sup>k</sup>
(Dy/Yb) <sub>N</sub>	1.20–1.59	1.59±0.23	1.25±0.17	1.10±0.25	1.12±0.11	1.37±0.05	1.15–1.51 (1.27±0.11)	1.08–1.34 (1.19±0.11)	0.96–1.20 (1.07±0.12)	1.20±0.13	0.8–1.1 <sup>l</sup>
Er/Nd	0.05–0.09	0.06±0.02	0.07±0.02	0.25±0.17	0.11±0.02	–	0.12–0.19 (0.2±0.03)	0.13–0.20 (0.2±0.02)	0.12–0.19 (0.1±0.02)	0.15±0.03	0.27 <sup>n</sup>
CaCO <sub>3</sub> %	42.27–66.53	88±5	75±15	–	51±22	47–87 Avg. 65.3	46.11–87.91 (75.8±13.31)	71.79–88.73 (81.9±6.82)	52.71–64.11 (61.5±10.66)	74.65±12.89	–
Eu/Eu*	0.84–1.43	0.78±0.31	0.58±0.11	–	1.15±0.08	>1	0.95–1.7 (1.28±0.95)	1.09–3.69 (1.88±1.009)	1.22–1.58 (1.41±0.15)	1.51±0.64	–
REE (ppm)	13.7–68.3	80±40	73±20	3.36±2.55	78±40	–	35.82±16.2	25.55±9.914	35.02±9.79	32.2±13.3	–
U	0.3–1.3	0.9±0.5	0.7±0.5	–	6±2	–	–	–	–	–	–
U/Th	0.12–1.25	0.19±0.10	0.22±0.29	–	2.1±0.5	–	–	–	–	–	–

<sup>a</sup>Armstrong-Altrin et al. 2003 (*n* = 9); <sup>b</sup>Madhavaraju and Ramasamy 1999; Late Cretaceous (*n* = 8); <sup>c</sup>Mazumdar et al. 2003; Late Neoproterozoic (*n* = 15); <sup>d</sup>Nath et al. 1997 (*n* = 9); <sup>e</sup>Nath et al. 1992; <sup>f</sup>Nagarajan et al. (2011) (*n* = 18); <sup>g</sup>Elderfield and Greaves 1982; Piegras and Jacobsen 1992; <sup>h</sup>De Baar et al. 1985; and Zhang and Nozaki 1996 respectively; <sup>i</sup>50 m water depth samples); <sup>j</sup>Webb and Kamber 2000; <sup>k</sup>Bau and Dulski 1996; <sup>l</sup>De Baar et al. 1988; <sup>n</sup>This study (Kajrahat Limestone)



typically lower compared to clastic sediments. Seawater contributes lesser amount of REE to the chemical sediments but the samples with non-seawater like pattern exhibits higher REE concentration (Nothdurft et al. 2004) due to the contamination of non-carbonate materials such as silicates, Fe–Mn oxides, phosphates or sulfides during the chemical leaching (Zhao et al. 2009). The higher REE concentrations in clastic sediments primarily result from the presence of silt and clay fractions. This occurs because REEs are readily being incorporated into the clay structure (McLennan 1989). The variation in the REE contents of Kajrahat Limestone may be attributed to the varying amounts of terrigenous sediments present. The lower REE content in some samples may be attributed to REE dilution by carbonate minerals.

The average  $(La/Yb)_N$  ratio in the studied limestone samples (0.98–2.13) is similar to the shallow-marine carbonates of southern India, Kudankulam Limestone. However,  $(La/Yb)_N$  ratios are lower in the studied limestones than observed in Arabian Sea carbonate sediments, Indian Ocean carbonates and Shahabad Formation Limestone (Table 5). Additionally, the  $(La/Yb)_N$  ratio is higher than the commonly assumed average value for terrigenous sediments [ $(La/Yb)_N = 1.3$ ; Sholkovitz 1990]. The  $(La/Yb)_N$  ratios variation in different samples could be attributed to two factors: (1) variations in REEs input from the source area; and (2) potential diagenetic processes leading to remobilization and exchange with interstitial water (Murray et al. 1991), alongside a decreasing trend of the  $(La/Yb)_N$  ratio with increasing depth (Worash and Valera 2002). Such diagenetic processes which is responsible for variation of  $(La/Yb)_N$  ratio have been reported in recent, shallow, buried estuaries (Sholkovitz et al. 1989). The present study resembles shallow-marine conditions where REE fractionation should have been low.

REE patterns and  $(La/Yb)_N$  ratios can be used to identify the characteristics of source rocks. Additionally, specific trace-element ratios like Th/Sc, La/Sc, and La/Th can provide valuable information about the source rocks characteristics, as these ratios are influenced by the average compositions of the provenance. Th is considered a highly incompatible element, while Sc is somewhat more compatible. During the sedimentation processes, both of these elements are transferred relatively uniformly into terrigenous sediments as they are transported from their source areas and deposited (Taylor and McLennan 1985). The studied limestone samples show a slightly enriched light rare earth elements (LREEs) and flat heavy rare earth elements (HREEs) patterns (Fig. 5). Additionally, they have relatively high average ratios of  $(La/Yb)_N$ , Th/Sc, La/Sc and La/Th (1.48, 0.68, 2.45 and 3.78, respectively; Table 3) which are comparable to felsic rocks (Nagarajan et al. 2011). The felsic source rock for terrigenous sediments of the studied samples also confirmed by the positive correlation between  $Eu/Eu^*$

and K/Al, Na/Al. These findings suggest that the terrigenous sediments within the shallow-marine Kajrahat Limestone originate predominantly from felsic source rocks.

### Europium anomaly

The  $Eu/Eu^*$  ratio of the studied limestone samples ranges from 0.84 to 1.43, (Table 3). Typically, a dearth of negative Eu anomaly and the presence of a positive Eu anomaly in shale-normalized REE patterns can be attributed to the influence of eolian input (Elderfield 1988) or hydrothermal solutions (Michard et al. 1983; Worash and Valera 2002). Positive Eu anomalies in bulk sediments may arise from a small increase in the primary or detrital feldspar component (Murray et al. 1991). The presence of a positive Eu anomaly in some studied limestone samples (KJ5, KJ1, LB10) (Table 3) suggests that it could be attributed to local feldspar enrichment rather than a regional phenomenon such as eolian input or hydrothermal solutions. The correlation between  $Eu/Eu^*$  and elemental ratios such as K/Al and Na/Al provides support for this interpretation, which helps to determine the existence of detrital feldspar in the bulk sediments (Madhavaraju and Lee 2009). Based on the results of this study, a strong positive correlation exists between the K/Al and Na/Al ratios and the  $Eu/Eu^*$  ( $r^2 = 0.73$ ,  $r^2 = 0.88$ ), respectively. This suggests that the presence of feldspars in these limestones could be the reason behind the observed positive Eu anomaly. This interpretation was strengthened by the high enrichment of Sr in studied samples (Table 2, Fig. 6). Eu is one of the REE shows a changing valency in the near surface environment (Brookins 1989), where  $Eu^{3+}$  reduced to  $Eu^{2+}$  under extremely reducing conditions. Redox potential of  $Eu/Eu^*$  in aqueous solutions depends mainly

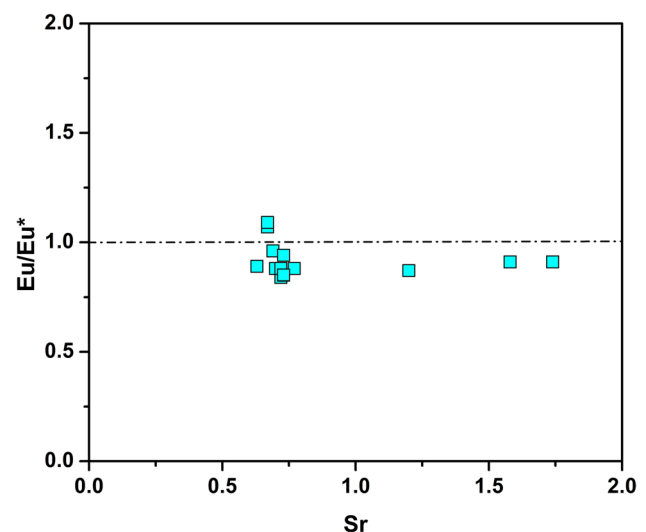


Fig. 6 Bivariate plot of  $Eu/Eu^*$  versus Sr for the Kajrahat Limestone

on temperature and to a lesser extent on pressure, pH, and REE speciation (Bau 1991); which explains the positive Eu anomalies typically found in acidic, reducing hydrothermal fluids. Additionally, the presence of negative Eu anomaly suggests the oxic depositional environment.

### Cerium anomaly and paleo-redox conditions

Several studies have been conducted the use of the Cerium (Ce) within the marine environments to infer paleoceanographic conditions (Liu et al. 1988; Grandjean and Albarede 1989; German and Elderfield 1990; Nath et al. 1997). The depletion of Ce in oceanic water result in redox-related fluctuations in cerium concentration compared to other REEs (Elderfield 1988; Piepgras and Jacobsen 1992). In modern seawater, a distinctive feature is the lower concentration of Ce in comparison to its neighbouring rare earth elements (REEs). This anomaly is caused by the conversion of trivalent Ce into less soluble tetravalent Ce due to oxidation. Subsequently, these trivalent Ce ions are removed as they bind to suspended particles that sink through the water column, a process known as scavenging (Bolhar et al. 2004). The Ce/Ce\* ratios within the examined limestones range from 0.66 to 0.89, with an average of 0.79. The consistent Ce anomalies in these limestones indicate a relatively stable level of oxygen in the bottom water during their deposition. The negative Ce anomalies observed in the studied limestones (Table 5) closely resemble those found in deep-sea carbonates from the Indian Ocean (Nath et al. 1992), Arabian Sea sediments (Nath et al. 1997), and shallow-marine Maastrichtian carbonates from the Cauvery Basin in southern India (Madhavaraju and Ramasamy 1999). The presence of both Ce concentrations and Ce anomalies is likely attributed to differences in terrigenous sediments within the studied limestones, as well as other factors like diagenesis.

Negative Ce anomalies are predominantly found in ocean basins due to absence of Ce in seawater, as Ce<sup>4+</sup> are selectively eliminated from the water column (Elderfield and Greaves 1982). The presence of a slight Ce anomaly allows for the measurement and representation of the extent of the La anomalies, which can be observed as a negative anomaly (Zhao et al. 2009). It is best to utilize a bivariate plot to properly analyze and discriminate between Ce and La anomalies (Bau and Dulski 1996; Zhao et al. 2009). The studied limestone samples represented in the discrimination diagram (Pr/Pr\* vs. Ce/Ce\*, Fig. 7) indicates that these samples display original negative Ce anomalies. As there is no chemical explanation for the formation of Nd or Pr anomalies, the presence of a true Ce anomaly should result in Pr/Pr\*  $\geq$  1. The range of Pr/Pr\* (1.06–1.24) in the studied samples indicates that the anomalous enrichment of La is likely the only factor contributing to any Ce anomaly. The degree of Ce

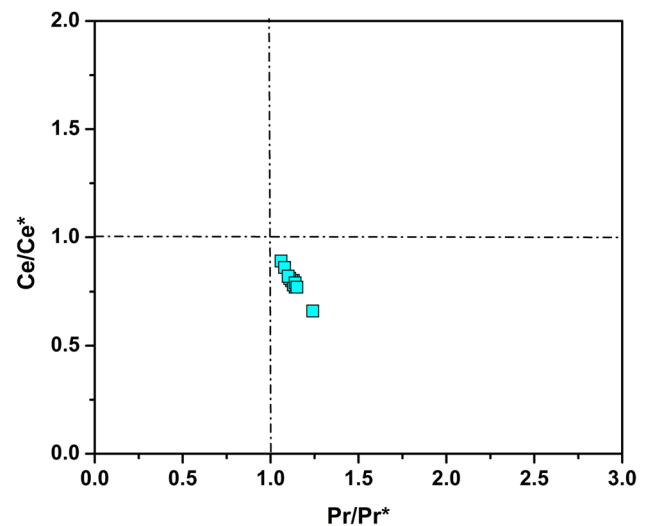


**Fig. 7** Bivariate plot of Ce/Ce\* versus Pr/Pr\* for the Kajrahat Limestone

depletion in the samples is a reflection of oxygenation level of the water (Komiya et al. 2008).

The findings of the present study indicate that the Kajrahat Limestone exhibits negative Ce anomalies, indicating that it was formed in an oxygen-rich environment. Furthermore, minimal Ce anomalies variation within these limestones, suggests stable bottom water oxygen levels. The differences in Ce anomalies and Ce concentrations within the limestone samples are likely a result of variations in terrigenous sediments rather than diagenesis.

### Conclusions

On the basis of detailed study of the major, trace and rare earth elements (REEs) geochemistry of carbonate rocks from the Palaeoproterozoic Kajrahat Limestone, Vindhyan Supergroup, Central India, the following conclusions were made:

1. The studied limestones are calcitic in nature with dominance of CaO. SiO<sub>2</sub> present as second most abundant major oxide. The enrichment of certain trace elements such as Ba, V, Cu, Rb, Zn and Zr may be due to the siliciclastic input.
2. The PAAS-normalized REE pattern exhibits a relatively uniform pattern characterized by enriched LREE, a negative Ce anomaly, a negative Eu anomaly and a low U/Th ratio. Variations in the abundance patterns of both LREE and HREE, as well as the variability observed in shale-normalized elemental ratios, are likely a result of varying contamination from continental material and

early diagenetic process that occurred in the carbonate sediments.

3. The REE patterns and ratios, including La/Sc, La/Th, Th/Sc and (La/Yb)<sub>N</sub> collectively indicate that the terrigenous sediments within the studied limestones predominantly originated from felsic source rocks.
4. The consistent presence of low U content and a low U/Th ratio indicates that oxic conditions were predominant at the sediment/water interface during the deposition of the Kajrahat Limestone. The presence of a negative Ce anomaly suggests that REEs are directly incorporated from seawater or from pore water in oxygen-rich conditions. This suggests a mixing of two-component systems, including terrigenous clay (detrital), within the marine sediments.
5. Tectonic environment of the basin played major role for geochemical pattern of the present studied limestones.

**Acknowledgements** Authors are thankful to the Director, Wadia Institute of Himalayan Geology for permitting to carry out chemical analysis of limestone samples.

**Author contributions** AS carried out fieldwork, conception and design of the study, data analysis, and drafting of the original manuscript. BPS reviewed and edited the manuscript and provided overall supervision. SK carried out fieldwork, conception and design of the study, data analysis, and drafting of the original manuscript. MAQ conception and design of the study and drafting of the original manuscript. AP carried out fieldwork, conception and designed the work and contributed in the finalisation of manuscript. SS drafting of the original manuscript. VKS improved and revised the manuscript.

**Data availability** All the data generated or analyzed during the present study are included in this manuscript.

## Declarations

**Conflict of interest** The authors declare that they have no competing interests.

## References

- Anderson R, Bacon MP, Brewer PG (1983) Removal of <sup>230</sup>Th and <sup>234</sup>Pb at ocean margins. *Earth Planet Sci Lett* 66:73–90
- Anderson RF, Lehuray AP, Fleisher MQ, Murray JW (1989) Uranium deposition in saanich inlet sediments, Vancouver Island. *Chem Geol* 53(9):2205–2213
- Ansari AH, Pandey SK, Sharma M, Agrawal S, Kumar Y (2018) Carbon and oxygen isotope stratigraphy of the Ediacaran Bilara Group, Marwar Supergroup, India: evidence for high amplitude carbon isotopic negative excursions. *Precamb Res* 308:75–91
- Armstrong-Altrin JS, Verma SP, Madhavaraju J, Lee YI, Ramasamy S (2003) Geochemistry of Late Miocene Kudankulam limestones, South India. *Int Geol Rev* 45:16–26
- Auden JB (1933) Vindhyan sedimentation in the Son Valley, Mirzapur District. *Mem Geol Sur India* 62:141–250
- Azmi RJ, Joshi D, Tiwari BN, Joshi MN, Srivastava SS (2008) A synoptic view on the current discordant geo- and biochronological ages of the Vindhyan Supergroup, central India. *Him Geol* 29(2):177–191
- Bakkiaraj D, Nagendra R, Nagarajan R, Armstrong-Altrin JS (2010) Geochemistry of Siliciclastic rocks of Sillakkudi Formation, Cauvery Basin, Southern India; implications for provenance. *J Geol Soc India* 76:453–467
- Banerjee S, Bhattacharya SK, Sarkar S (2007) Carbon and oxygen isotopic variations in peritidal stromatolite cycles, Paleoproterozoic Kajrahat limestone, Vindhyan Basin of central India. *J Asian Earth Sci* 29:823–831
- Banner JL, Hanson GN (1990) Calculation of simultaneous isotopic and trace element variations during water-rock interaction with applications to carbonate diagenesis. *Geochim Cosmochim Acta* 54:3123–3137
- Banner JL, Hanson GN, Meyers WJ (1988) Water-rock interaction history of regionally extensive dolomites of the Burlington-Keokuk Formation (Mississippian): isotopic evidence. In: Shukla V, Baker P (eds) *Sedimentology and Geochemistry of Dolostones*, vol 43. SEPM Spec Pub, Tulsa, pp 97–114
- Bau M (1991) Rare-earth element mobility during hydrothermal and metamorphic fluid-rock interaction and the significance of the oxidation state of europium. *Chem Geol* 93:219–230
- Bau M, Dulski P (1996) Anthropogenic origin of positive gadolinium anomalies in river waters. *Earth Planet Sci Lett* 143:245–255
- Bickford ME, Mishra M, Mueller PA, Kamenov GD, Schieber J, Basu A (2017) U-Pb age and Hf isotopic compositions of magmatic zircons from a rhyolite flow in the Porcellanite Formation in the Vindhyan Supergroup, Son Valley (India): Implications for its tectonic significance. *J Geol* 125:367–379
- Birgel D, Feng D, Roberts HH, Peckmann J (2011) Changing redox conditions at cold seeps as revealed by authigenic carbonates from Alaminos Canyon, northern Gulf of Mexico. *Chem Geol* 285(1):82–96
- Bolhar R, Kranendonk MJV (2007) A non-marine depositional setting for the northern Fortescue Group, Pilbara Craton, inferred from trace element geochemistry of stromatolitic carbonates. *Precamb Res* 155:229–250
- Bolhar R, Kamber BS, Moorbath S, Fedo CM, Whitehouse MJ (2004) Characterisation of early Archaean chemical sediments by trace element signatures. *Earth Planet Sci Lett* 222:43–60
- Bose PK, Banerjee S, Sarkar S (1997) Slope-controlled seismic deformation and tectonic framework of deposition; Koldaha Shale, India. *Tectonophysics* 269:151–169
- Bose PK, Sarkar S, Chakraborty S, Banerjee S (2001) Overview of the Meso to Neoproterozoic evolution of the Vindhyan Basin, central India. *Sediment Geol* 141:395–419
- Brand U, Veizer J (1980) Chemical diagenesis of a multi component carbonate system: 1. Trace elements. *J Sediment Petrol* 50:1219–1236
- Brookins DG (1989) Aqueous geochemistry of rare earth elements. In: Lipin BR and McKay GAŽ (eds) *Geochemistry and Mineralogy of Rare Earth Elements*. *Rev Mineral Geochem* 21:201–225
- Chanda SK, Bhattacharyya A (1982) Vindhyan sedimentation and paleogeography: Post-Auden developments. In: Valdiya KS, Bhatia SB, Gaur VK (eds) *Geology of Vindhyan*. Hindustan Publishing Corporation, Delhi, India, pp 88–101
- Chaudhuri S, Cullers RL (1979) The distribution of rare earth elements in deeply buried Gulf coast sediments. *Chem Geol* 24:327–338
- Choudhuri A, Albani AEI, Mandal S, Sarkar S (2023) Biotic vs abiotic origin of unusual features from Mesoproterozoic of Vindhyan Supergroup India. *Annales De Paleontologie* 109(3):102629
- Coimbra R, Immenhauser A, Olóriz F, Rodríguez-Galiano V, Chicla-Olmo M (2015) New insights into geochemical behaviour in ancient marine carbonates (Upper Jurassic Ammonitico Rosso): Novel proxies for interpreting sea-level dynamics and palaeoceanography. *Sedimentology* 62(1):266–302

- de Baar HJ, Bacon MP, Brewer PG, Bruland KW (1985) Rare earth elements in the Pacific and Atlantic Oceans. *Geochim Cosmochim Acta* 49:1943–1959
- de Baar HJ, German CR, Elderfield H, Van Gaans P (1988) Rare earth element distributions in anoxic waters of the Cariaco Trench. *Geochim Cosmochim Acta* 52:1203–1219
- Deb M, Thorpe R, Krstic D (2002) Hindoli group of rocks in the eastern fringe of the Aravalli-Delhi orogenic belt-archean secondary greenstone belt or proterozoic supracrustals. *Gond Res* 5:879–883
- Elderfield H (1988) The oceanic chemistry of the rare-earth elements. *Philos Trans Roy Soc London* 325:105–126
- Elderfield H, Greaves MJ (1982) The rare earth elements in seawater. *Nature* 296:214–219
- Elderfield H, Pagett R (1986) Rare earth elements in ichthyoliths: variations with redox conditions and depositional environments. *Sci Tot Env* 49:175–197
- Fairbridge RW (1972) *The Encyclopedia of Geochemistry and Environmental Sciences*. Van Nostrand Reinhold Company, New York
- Frimmel HE (2009) Trace element distribution in Neoproterozoic carbonates as palaeoenvironmental indicator. *Chem Geol* 258:338–353
- Fu X, Wang J, Zeng Y, Tan F, He J (2011) Geochemistry and origin of rare earth elements (REEs) in the Shengli River oil shale, northern Tibet, China. *Geochemistry* 71(1):21–30
- George BG, Ray JS, Shukla AD, Chatterjee A, Awasthi N, Laskar AH (2018) Stratigraphy and geochemistry of the Balwan Limestone, Vindhyan Supergroup, India: evidence for the Bitter Springs  $\delta^{13}\text{C}$  anomaly. *Precamb Res* 313:18–30
- German CR, Elderfield H (1990) Application of the Ce anomaly as a paleoredox indicator: the ground rules. *Paleoceanogr* 5:823–833
- Goldberg ED, Koide M, Schmitt RA (1963) Rare earth distributions in the marine environment. *J Geophys Res* 68:4209–4217
- Gong N, Hong H, Huff WD, Fang Q, Bae CJ, Wang C, Yin K, Chen S (2018) Influences of sedimentary environments and volcanic sources on diagenetic alteration of volcanic tuffs in South China. *Sci Rep* 8:7616
- Gopalan K, Kumar A, Kumar S, Vijaygopal B (2013) Depositional history of the Upper Vindhyan succession, central India: time constraints from Pb-Pb isochron ages of its carbonate components. *Precamb Res* 233:108–117
- Grandjean P, Albarède F (1989) Ion probe measurement of rare earth elements in biogenic phosphates. *Geochim Cosmochim Acta* 53(12):3179–3183
- Haskin MA, Haskin LA (1966) Rare earths in European shales, a redetermination. *Science* 154:507–509
- Holland HD (1984) *The chemical evolution of the atmosphere and oceans*. Princeton University Press, Series in Geochemistry, Princeton, New Jersey, p 582
- Holser WT (1997) Evaluation of the application of rare-earth elements to paleoceanography. *Palaeogeog Palaeoclim Palaeoeco* 132:309–323
- Jones B, Manning DC (1994) Comparison of geochemical indices used for the interpretation of paleo-redox conditions in Ancient mudstones. *Chem Geol* 111(1–4):111–129
- Kale VS, Phansalkar VG (1991) Purana Basins of Peninsular India: a review. *Basin Res* 3:1–36
- Kamber BS, Webb GE (2001) The geochemistry of late Archaean microbial carbonate: implications for ocean chemistry and continental erosion history. *Geochim Cosmochim Acta* 65:2509–2525
- Kato Y, Nakao K, Isozaki Y (2002) Geochemistry of Late Permian Triassic pelagic cherts from southwest Japan: implications for an oceanic redox change. *Chem Geol* 182:15–34
- Kemp RA, Trueman CN (2003) Rare earth elements in Soln-hofen biogenic apatite: geochemical clues to the palaeoenvironment. *Sedim Geol* 155:109–127
- Kochenov AV, Korolev KG, Dubinchuk VT, Medvedev YL (1977) Experimental data on the conditions of precipitation of uranium from aqueous solutions (translated from *Geokhimiya* 11:1711–1716). *Geochem Int* 82–87
- Komiya T, Hirata T, Kitajima K, Yamamoto S, Shibuya T, Sawaki Y, Ishikawa T, Shu D, Li Y, Han J (2008) Evolution of the composition of seawater through geologic time, and its influence on the evolution of life. *Gond Res* 14:159–174
- Kumar S (1978) On the Kheinjua Formation of Semri Group, Lower Vindhyan, Newari Area, Mirzapur District, U.P. *Proceed Ind Nat Sci Acad* 44A:144–154
- Langmuir D (1978) Uranium solution-mineral equilibrium at low temperatures with applications to sedimentary ore deposits. *Geochim Cosmochim Acta* 42:547–569
- Li ZX, Bogdanova SV, Collins AS, Davidson A, De Waele B, Ernst RE, Fitzsimons ICW, Fuck RA, Gladkochub DP, Jacobs J, Karlstrom KE, Lu S, Natapov LM, Pease V, Pisarevsky SA, Thrane K, Vernikovsky V (2008) Assembly, configuration, and break-up history of Rodinia: a synthesis. *Precamb Res* 160:179–210
- Liu YG, Miah MRU, Schmitt RA (1988) Cerium, a chemical tracer for paleo-oceanic redox conditions. *Geochim Cosmochim Acta* 52:1361–1371
- Madhavaraju J, Lee YI (2009) Geochemistry of the Dalmiapuram Formation of the Uttatur Group (Early Cretaceous), Cauvery basin, southeastern India: Implications on provenance and paleo-redox conditions. *Rev Mex De Cienc Geol* 26:380–394
- Madhavaraju J, Ramasamy S (1999) Rare earth elements in limestones of Kallankurichchi Formation of Ariyalur Group, Tiruchirapalli Cretaceous, Tamil Nadu. *J Geol Soc India* 54:291–301
- Malone S, Meert J, Banerjee DM, Pandit M, Tamrat E, Kamenov GD, Pradhan V, Sohl LE (2008) Paleomagnetism and detrital zircon geochronology of the Upper Vindhyan Sequence, Son Valley and Rajasthan, India: a ca. 1000Ma closure age for the Purana Basins. *Precamb Res* 164:137–159
- Martin JM, Whitfield M (1983) The significance of the river input of chemical elements to the ocean. *Trace Met Sea Water* 9:265–296
- Mazumdar A, Tanaka K, Takahashi T, Kawabe I (2003) Characteristics of rare earth element abundances in shallow marine continental platform carbonates of Late Neoproterozoic successions from India. *Geochem J* 37:277–289
- McLennan SM (1989) Rare earth elements in sedimentary rocks; influence of provenance and sedimentary processes. In: Lipin BR, McKay GA (eds.) *Geochemistry and Mineralogy of Rare Earth Elements*, *Rev Miner* 21:169–200
- Meert JG, Santosh M (2017) The Columbia supercontinent revisited. *Gond Res* 50:67–83
- Michard A, Albarède F, Michard G, Minister JF, Charlou JL (1983) Rare earth elements and uranium in high temperature solutions from East-Pacific Rise hydrothermal vent field (13°N). *Nature* 303:795–797
- Mohanty SP, Barik A, Sarangi S, Sarkar A (2015) Carbon and oxygen isotope systematics of a Paleoproterozoic cap-carbonate sequence from the Sausar Group, Central India. *Palaeogeog Palaeoclim Palaeoeco* 417:195–209
- Morad S, Al-Aasm IS, Sirat M, Sattar MM (2010) Vein calcite in Cretaceous carbonate reservoirs of Abu Dhabi: record of origin of fluids and diagenetic conditions. *J Geochem Explo* 106:156–170
- Muecke GK, Pride C, Sarkar P (1979) Rare earth element geochemistry of regional metamorphic rocks. *Phy Chem Ear* 11:449–464
- Murray RW (1994) Chemical criteria to identify the depositional environment of chert: general principles and applications. *Sediment Geol* 90:213–232



- Murray RW, Buchholtz MR, Brink MR, Jones DL, Gerlach DC, Russ GP III (1990) Rare earth elements as indicators of different marine depositional environments in chert and shale. *Geology* 18:268–271
- Murray RW, Buchholtz MR, Brumsack HJ (1991) Rare earth elements in Japan Sea sediments and diagenetic behaviour of Ce/Ce\*, results from ODP leg 127. *Geochim Cosmochim Acta* 55:2453–2466
- Murray RW, Buchholtz MR, Ten Brink MR, Gerlach DC, Russ GPIII, Jones DL (1992) Inter-oceanic variation in the rare earth, major and trace element depositional chemistry of chert: perspectives gained from the DSDP and ODP record. *Geochim Cosmochim Acta* 56:1897–1913
- Myers KJ, Wignall PB (1987) Understanding Jurassic organic-rich mudrocks—New concepts using gamma ray spectrometry and palaeoecology: examples from the Kimmeridge Clay of Dorset and the Jet Rock of Yorkshire. In: Legget JK (ed) *Marine clastic environments: concepts and case studies*. Graham and Trotman, London, pp 175–192
- Nagarajan R, Madhavaraju J, Armstrong-Altrin JS, Nagendra R (2011) Geochemistry of neoproterozoic limestones of the Shahabad Formation, Bhima Basin, Karnataka, southern India. *Geosci J* 15:9–25
- Nath BN, Roelands I, Sudhakar M, Plueger WL (1992) Rare earth element patterns of the Central Indian Basin sediments related to their lithology. *Geophy Res Lett* 19:1197–1200
- Nath BN, Bau M, Ramalingeswara Rao B, Rao ChM (1997) Trace and rare earth elemental variation in Arabian Sea sediments through a transect across the oxygen minimum zone. *Geochim Cosmochim Acta* 61:2375–2388
- Nichols G (2009) *Sedimentology and stratigraphy*, 2nd edn. Wiley, West Sussex, p 419
- Nogueira LB, Oliveira VQ, Araujo LP, Leao LP, Ali A, Leite MGP, Nalini HA Jr (2019) Geochemistry and C and O isotope composition of carbonate rocks from Bemil and Lagoa Seca quarries, Gandarela Formation, Quadrilátero Ferrífero – Brazil. *J South American Earth Sci* 92:609–630
- Nothdurft LD, Webb GE, Kamber BS (2004) Rare earth element geochemistry of Late Devonian reefal carbonates, Canning Basin, Western Australia: confirmation of a seawater REE proxy in ancient limestone. *Geochim Cosmochim Acta* 68:263–283
- Nozaki Y, Horibe Y, Tsubota H (1981) The water column distribution of thorium isotopes in the western North Pacific. *Earth Planet Sci Lett* 54:203–216
- Palmer MR (1985) Rare earth elements in foraminifera tests. *Earth Planet Sci Lett* 73:285–298
- Patra A, Singh BP (2017) Geochemistry of the Eocene limestones of the Jaisalmer Basin, Rajasthan, India: implications on depositional conditions and sources of rare earth elements. *Geochem Int* 55(12):1140–1152
- Piegras DJ, Jacobsen SB (1992) The behaviour of rare earth elements in seawater: precise determination of ferromanganese crusts. *Geochim Cosmochim Acta* 56:1851–1862
- Piper DZ (1974) Rare earth elements in ferromanganese nodules and other marine phases. *Geochim Cosmochim Acta* 38:1007–1022
- Ramakrishnan M, Vaidyanadhan R (2008) *Geology of India*. J Geol Soc India pp 556
- Rasmussen B, Bose PK, Sarkar S, Banerjee S, Fletcher IR, McNaughton NJ (2002) 1.6 Ga U-Pb zircon age for the Chorhat Sandstone, lower Vindhyan, India: possible implications for early evolution of animals. *Geology* 30:103–106
- Ray JS (2006) Age of the Vindhyan supergroup: a review of recent findings. *Earth Syst Sci* 115(1):149–160
- Ray JS, Martin MW, Veizer J, Bowing SA (2002) U-Pb zircon dating and Sr isotope systematic of the Vindhyan Supergroup India. *Geology* 30:131–134
- Ray JS, Veizer J, Davis WJ (2003) C, O, Sr and Pb isotope systematic of carbonate sequences of the Vindhyan Supergroup, India: age, diagenesis, correlation and implications for global events. *Precamb Res* 121:103–140
- Reeder RJ (1983) Crystal chemistry of the rhombohedral carbonates. *Mineral Soc Am Rev* 11:1–48
- Rollinson HS (1993) *Using geochemical data: evaluating, presentation, interpretation (chemistry series)*. Pearson Prentice Hall pp 384
- Sarangi S, Gopalan K, Kumar S (2004) Pb-Pb age of earliest megascopic, eukaryotic alga bearing Rohtas Formation, Vindhyan Supergroup, India: Implications for Precambrian atmospheric oxygen evolution. *Precamb Res* 132:107–121
- Scherer M, Seitz H (1980) Rare-earth element distribution in Holocene and Pleistocene corals and their distribution during diagenesis. *Chem Geol* 28:279–289
- Schieber J (1988) Redistribution of rare earth elements during diagenesis of carbonate rocks from Mid-Proterozoic Newland Formation, Montana, USA. *Chem Geol* 69:111–126
- Shields GA, Webb GE (2004) Has the REE composition of seawater changed over geologic time. *Chem Geol* 204:103–107
- Sholkovitz ER (1990) Rare earth elements in marine sediments and geochemical standards. *Chem Geol* 88:333–347
- Sholkovitz ER, Piegras DJ, Jacobsen SB (1989) The pore water chemistry of rare elements Buzzard Bay sediments. *Geochim Cosmochim Acta* 53:2847–2856
- Shukla AD, George BG, Ray JS (2020) Evolution of the Proterozoic Vindhyan Basin, Rajasthan, India: insights from geochemical provenance of siliciclastic sediments. *Int Geol Rev* 62(2):153–167
- Singh BP, Pawar JS, Patra A (2013) Geochemistry of Late Eocene/Oligocene calcrites (caliche) of the northwestern Himalaya, India. *J Him Earth Sci* 34(2):135–140
- Singh BP, Mondal K, Singh A, Mittal P, Singh RK, Kanhaiya S (2020) Seismic origin of the soft-sediment deformation structures in the upper Palaeo-Mesoproterozoic Semri Group, Vindhyan Supergroup. *Central India Geol J* 55(11):7474–7488
- Srivastava VK, Singh BP (2018) Depositional environments and sources for the middle Eocene Fulra Limestone Formation, Kachchh Basin, western India: evidences from facies analysis, mineralogy, and geochemistry. *Geol J* 54(1):62–82
- Takematsu N, Sato Y, Kato Y, Okabe S (1993) Factors regulating the distribution of elements in marine sediments predicted by a simulation model. *J Oceanogr* 49(4):425–441
- Taylor SR, McLennan SM (1985) *The continental crust: Its composition and evolution*. Blackwell Scientific, Oxford, p 312
- Tlig S, M'Rabet A (1985) A comparative study of the Rare Earth element (REE) distributions within the lower Cretaceous dolomites and limestones of Central Tunisia. *Sedimentology* 32:897–907
- Toyoda K, Nakamura Y, Masuda A (1990) Rare earth elements of Pacific pelagic sediments. *Geochim Cosmochim Acta* 54:1093–1103
- Wang YL, Liu YG, Schmitt RA (1986) Rare earth element geochemistry of south Atlantic deep sediments, Ce anomaly change at ~54 MY. *Geochim Cosmochim Acta* 50:1337–1355
- Webb GE, Kamber BS (2000) Rare earth elements in Holocene reefal microbialites: a new shallow seawater proxy. *Geochim Cosmochim Acta* 64:1557–1565
- Whittaker SG, Kyser TK (1993) Variations in the neodymium and strontium isotopic composition and REE content of molluscan shells from the Cretaceous Western Interior Seaway. *Geochim Cosmochim Acta* 57:4003–4014
- Wignall PB, Twitchett RJ (1996) Oceanic anoxia and the end Permian mass extinction. *Science* 272:1155–1158
- Worash G, Valera R (2002) Rare earth element geochemistry of the Antalo Super sequence in the Mekele Outlier (Tigray region, northern Ethiopia). *Chem Geol* 182(2–4):395–407

- Wright J, Seymour RS, Shaw HF (1984) REE and neodymium isotopes in conodont apatite. Variation with geological age and depositional environment. *Geol Soc Am Spec Paper* 196:325–340
- Yang NS, Guo Y, Yue W, Wang X, Yin P, Huang X (2017) Revisit of rare earth element fractionation during chemical weathering and river sediment transport. *Geochem Geophys Geosys* 18(3):935–955
- Zhang J, Nozaki Y (1996) Rare earth elements and yttrium in seawater: ICP-MS determinations in the East Caroline, Coral Sea, and South Fiji basins of the western South Pacific Ocean. *Geochim Cosmochim Acta* 60:4631–4644
- Zhang K, Shields GA (2023) Early diagenetic mobilization of rare earth elements and implications for the Ce anomaly as a redox proxy. *Chem Geol* 635:121619
- Zhang KJ, Li QH, Yan LL, Zeng L, Lu L, Zhang YX, Hui J, Jin X, Tang XC (2017) Geochemistry of limestones deposited in various plate tectonic settings. *Earth Sci Rev* 167(28):27–46
- Zhao YY, Zheng YF, Chen F (2009) Trace element and strontium isotope constraints on sedimentary environment of Ediacaran carbonates in southern Anhui, South China. *Chem Geol* 265:345–362
- Zhong S, Mucci A (1995) Partitioning of rare earth elements (REEs) between calcite and seawater solutions at 25 °C and 1atm, and high dissolved REE concentrations. *Geochim Cosmochim Acta* 59:443–453

**Publisher's Note** Springer Nature remains neutral with regard to jurisdictional claims in published maps and institutional affiliations.

Springer Nature or its licensor (e.g. a society or other partner) holds exclusive rights to this article under a publishing agreement with the author(s) or other rightsholder(s); author self-archiving of the accepted manuscript version of this article is solely governed by the terms of such publishing agreement and applicable law.